# Computer-aided Framework Design for Digital Dentistry

Hong-Tzong Yau[1], Chien-Yu Hsu[2], Hui-Lang Peng[3] and Chih-Chuan Pai[4]

[1,2]National Chung-Cheng University, [1]imehty@ccu.edu.tw, [2]apache@pcc-server.ccu.edu.tw
[3,4]Pou-Yuen Technology, [3]bhl@pcc-server.ccu,.edu.tw, [4]alexbai@pcc-server.ccu.edu.tw

## ABSTRACT

The aim of this paper is to propose a customized dental framework (coping) design system to improve artificial teeth production. First, a structure light optical scanner is used to scan the teeth model. And the registration and triangulation algorithms are used to reconstruct the scanned data to a triangular solid model. In the coping design process, the first part is to find the margin lines of the prepared abutment teeth. Then the non-uniform offsetting and shelling algorithm is proposed to create the coping shell model with variable thickness. When restoring an edentulous space with a fixed partial denture that will crown the teeth adjacent to the space and bridge the gap with a pontic the restoration is referred to as a bridge. When the size or shape of coping and pontic models are not correct, some deformation tools are proposed to edit manually. Finally, the connector will be created between coping and pontic models.

**Keywords:** dental CAD/CAM, coping design, dental bridge, porcelain-fused-to-metal crown.
**DOI:** 10.3722/cadaps.2008.667-675

## 1. INTRODUCTION

CAD/CAM technology in the matter of fact helps in design and development of three-dimensional models and their realization on numerical controlled machines. The earliest attempt to apply CAD/CAM technology to dentistry began in the 1970s with Bruce Altschuler in the United States, Francois Duret in France, and Werner Mormann and Marco Brandestini in Switzerland [24]. Traditionally, the teeth to be crowned are prepared by a dentist and records are given to a dental technician to fabricate the crown or bridge, which can then be inserted at another dental appointment. Full-porcelain (ceramic) restorations are particularly desirable because their color and translucency mimic natural tooth enamel. Another type is known as porcelain-fused-to-metal (Fig. 1(b)), which is used to provide strength to a crown or bridge. Porcelain-fused-to-metal (PFM) crowns consist of a metal coping that is made by lost-wax casting technique (Fig. 1(a)) and primed for an application of porcelain. These restorations are very strong, durable and resistant to wear, because the combination of porcelain and metal creates a stronger restoration than porcelain used alone.

As new technology and material chemistry (zirconium-oxide) has evolved, computers are increasingly becoming a part of crown and bridge fabrication, such as in CAD/CAM technology. Traditionally, once a tooth is prepared for a crown, a cast is made and sent to a laboratory, where a coping is produced by manual techniques. With a contact or optical scanner, the cast is scanned in the lab where a coping is made by computer-directed machines to exact specifications of the original scanned casting.

This paper proposes a customized dental coping design system to improve coping production. First, a structure light optical scanner is used to scan the teeth model. And the registration and triangulation algorithms are used to reconstruct the scanned data to a triangular solid model. In the coping design process, the first part is to find the margin lines of the prepared abutment teeth. The root surface of the abutment teeth can be segmented according to these margin lines. Then the non-uniform offsetting and shelling algorithm is proposed to create the coping shell model with variable thickness. When restoring an edentulous space with a fixed partial denture that will crown the teeth adjacent to the space and bridge the gap with a pontic, or "dummy tooth", the restoration is referred to as a bridge. The system can load the pontic model from the database automatically. When the size or shape of coping and pontic

models are not correct, some deformation tools are proposed to edit manually. Finally, the connector will be created between coping and pontic models.



|         (a)          |           (b)            |

Fig. 1: (a) Dental plaster model with wax coping model (b) Dental plaster model with porcelain-fused-to metal crown.

## 2. PREVIOUS WORK

There has been many works done in the past on developing techniques for the dental CAD/CAM system and triangular model editing. We will discuss just a few recent publications and papers that describe those techniques which are close to ours system.

### 2.1 Dental CAD/CAM System

In [24], it provides an overview of the development of various CAD/CAM systems. Operational components, methodologies, and restorative materials used with common CAD/CAM systems are discussed. The CEREC system [19] is the world's first and only chair-side CAD/CAM restorative procedure. It could be a simple filling, an in-lay or a full crown, depending on how much healthy tooth structure is remaining. The Procera system [20] uses patented CAD/CAM technology to improve coping production. The DCS Precident system [18] is comprised of a laser scanner and Precimill CAM multi-tool milling center. The DCS Dentform software [18] automatically suggests connector sizes and pontic forms for bridges.

### 2.2 Point Cloud Data Set Registration and Triangulation

The Iterative Closest Point Algorithm (ICP) has become established as one the most useful methods of range data processing. Given two sets of partially overlapping range data and an initial estimate of their relative positions, ICP is used to register the data sets by improving the position and orientation estimate. First described by Besl and McKay [15], ICP is an essential step in model building, dimensional inspection, and numerous applications of range data processing [2-6].

Many algorithms based on triangulated surfaces have been proposed to reconstruct surfaces with arbitrary topology [7]. The early volume-based reconstruction method of Boissonnate [8], the well-known $\alpha$-shapes of Edelsbrunner et al. [8], the $\lambda$-complex of Adamy [9], the crust and power crust algorithms of Amenta et al. [10], and the adaptive sculpting algorithm of Yau and Kuo [11, 12] generally fall into this category.

### 2.3 Triangular Model Editing

Free-form deformation [16] is a well know modeling tool, but controlling the shape of an object under complex deformation is difficult. In [17], it proposes a modified FFD that uses B-spline basis in stead of the Bernstein polynomials because of the local control properties. In [21][22], by sketching the desired deformation of this reference curve, the user can implicitly and intuitively control the deformation of an entire region of the surface. An approach to define shape deformations by constructing and interactively modifying $C^1$ continuous time-dependent divergence-free vector fields is presented in [23].

## 3. DENTAL MODEL DIGITIZNG

To digitize dental plaster models, a structure light optical scanner (Fig. 2) is used to scan the teeth model in various directions, resulting in several sets of scan data in different coordinate systems. Then a registration process [2, 15] can be used to align these data sets so that they are all in the same coordinate system.

These data sets can be viewed as data patches now needed to be integrated together to form a complete solid model. However, gaps or holes can exist between different data patches. Overlaps also exist between adjacent data patches. In

current practice, it takes much labor to manually edit and stitch the gaps and holes using commercial software packages. With the proposed approach, the stitching and integration process can be highly automated. The proposed process for the stitching of multiple scan data sets is outlined by the following three steps:

Step 1: registration of multiple scan data sets.

Step 2: removal of overlapped data set.

Step 3: reconstruction of an STL solid model from the complete data set.

The registration problem can be defined as follows: "Given two sets of three-dimensional scan data viewed from different coordinate systems, find the spatial transformation between the two sets of data so that they can be properly matched in space." Here, let P and Q represent the characteristic points, and P and Q are two data sets of $\{p_i\}_{i=1\sim N}$ and $\{q_i\}_{i=1\sim N}$ respectively. The registration of the two data sets P and Q is an optimization problem and can be formulated as follows:

$$F(R,T) = \sum_{i=1}^{N}[Rp_i + T - NearestPt(p_i)]^2 \tag{1}$$

where $F$ is the objective function; $R$ and $T$ are the rotation and translation matrices that transform $p_i$ to match $q_i$; $NearestPt(p_i)$ represents a point in $\{q_i\}$ that is nearest to $p_i$. For a more detailed description of the registration algorithm, one can refer to [2, 15].

After two data sets P and Q are aligned, the point density in the overlapped region is obviously higher. For the purpose of uniform point distribution, we can keep one data set and remove the other part of the data set in the overlapped region. Let Q be the reference data set which will be kept, and P be the corresponding data set, of which the points in the overlapped region will be deleted. The remaining points in P are represented by a data set called P'. To find the points of P in the over lapped region, a user-defined overlapped distance $od$ is defined first. Given a value of $od$, point $p_k$ is regarded as an overlapped point in P if the projection distance from $p_k$ to Q is less than $od$. However, the projection of a point to a dense triangular mesh can be computationally costly. Therefore, in our implementation, a three-dimensional $k$-D tree of Q is built first. A bounding box centered at $p_k$ is created, with the side length equal to 2 $od$. Using the quick search of the $k$-D tree, one can very efficiently find if there is any point that belongs to Q inside the bounding box. If the answer is positive, then $p_k$ is determined to be an overlapped point. Although the overlapped distance is user-defined, it can be assigned equal to the scanning pitch which can be appropriately estimated from the scan data.

Based on the above definition, the overlapped points of P and Q can be quickly identified by employing a $k$-D tree data structure. After the overlapped points are identified, an integrated data set with uniform point distribution can be obtained by simply adding P' and Q.

Repeating steps 1 and 2 until all data sets have been aligned, we finally obtain a complete data set with uniform point distribution. With the adaptive *DBRG* algorithm [13] of surface reconstruction, the stitching of an STL solid model from multiple scan data becomes intuitive and straightforward. Simply take all points of the above complete data set as the input sample points *S* of the reconstruction algorithm.

The output will be the expected STL solid model. Even if there exist holes or gaps in the scan data, the adaptive *DBRG* algorithm automatically performs hole filling and gap stitching.

## 4. DESIGN TOOLS

After digitizing the dental plaster model, the dental coping model can be designed in the proposed system. In the coping design process, the first part is to find the margin lines of the prepared abutment teeth. The root surface of the abutment teeth can be segmented according to these margin lines. Then the non-uniform offsetting and shelling algorithm is proposed to create the coping shell model with variable thickness. When restoring an edentulous space with a fixed partial denture that will crown the teeth adjacent to the space and bridge the gap with a pontic the restoration is referred to as a bridge. The system can load the pontic model from the database automatically. When the size or shape of coping and pontic models are not correct, some deformation tools are proposed to edit the model manually. Finally, the connector will be created between coping and pontic models. The flowchart is shown in Fig. 3.
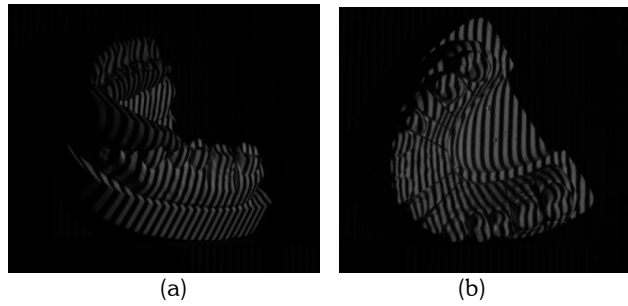
(a)           (b)

Fig. 2: To scan dental plaster model by using the structure light optical scanner in different directions.
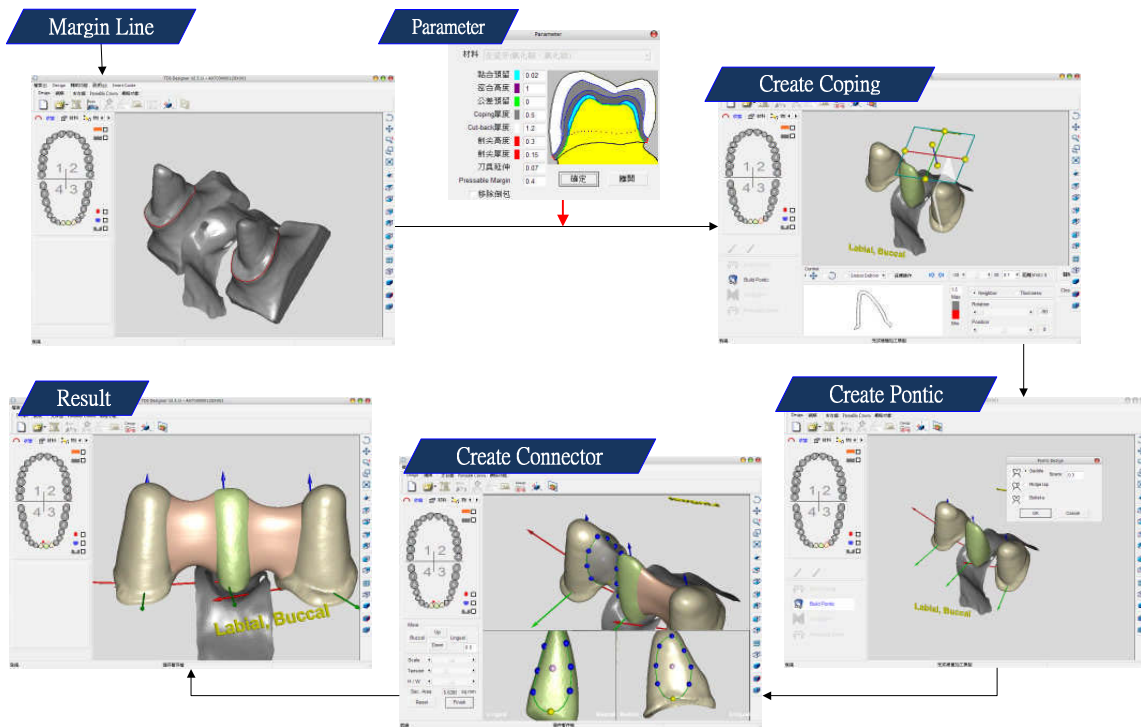


Fig. 3: The flowchart of the coping design system.

### 4.1 Margin Line Extraction

The second order difference is used to find the feature area. It assigns a weight to every edge in the mesh proportional to the dihedral angle defined by the normal of its two adjacent triangles. The idea is based on the second order difference operator constructed in [14], which was used to fair meshes of arbitrary connectivity. The operator is locally bound and can be evaluated efficiently.

$$w(e) = \cos^{-1}\left(\frac{n_i}{\|n_i\|}\frac{n_j}{\|n_j\|}\right) \tag{2}$$

The variables $n_i$ and $n_j$ correspond to the normal of the two triangles that share edge $e$.

When the feature patches are computed, we use a skeleton algorithm presented in [13]. The patches are thinned to a set of mesh features by burning the edges from the boundary of the patches down to a set of piecewise linear curves. In Fig. 4, the margin line are extracted automatically and the root surface area of the abutment can be segmented
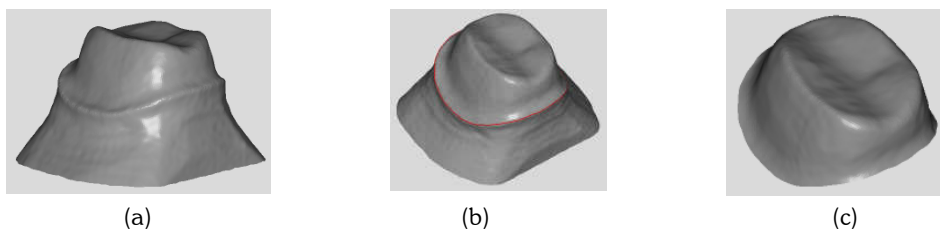
according to the margin line.



(a)                                   (b)                                   (c)

Fig. 4: The margin line extraction and the segmentation of the root surface area.

## 4.2 Non-uniform Offsetting and Shelling Algorithm

The idea of our proposed approach is from the concept of medial axis in computational geometry. The media axis method will not have self-intersection problem like other heuristic approaches. The offsetting points can be calculated with variable distance and the shelling model is reconstructed from these unorganized points by using triangulation algorithm proposed in [12].

The proposed process for the non-uniform offsetting and shelling algorithm is outlined by the following three steps:

Step 1: handling interference problem by using poles (for concave region)

Step 2: handling offsetting precision by inserting points (for convex region)

Step 3: surface reconstruction [12]

In Fig.5 (b) , the parameters of the non-uniform offsetting are input to create the dental coping model after margin line extraction. The offsetting area with different distance can be selected manually (Fig. 5 (c)). The dental coping model with variable offsetting distance is shown in Fig. 5 (d).
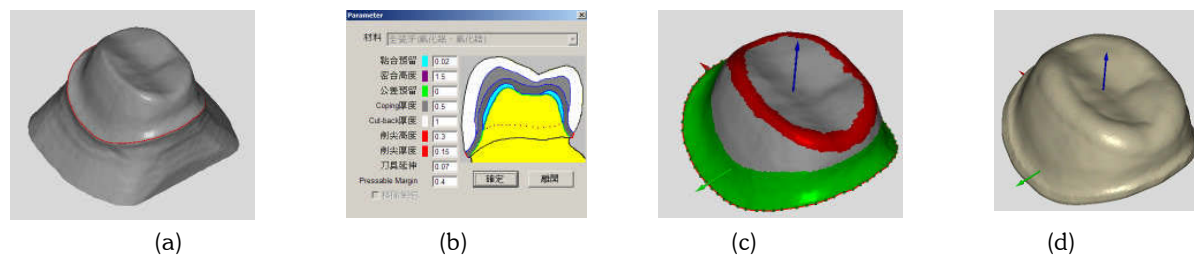


(a)                          (b)                          (c)                          (d)

Fig. 5: The coping model created by non-uniform offsetting and shelling algorithm.

## 4.3 Pontics

The pontic models are pre-constructed and saved in the database. The program will load the pontic model from the database automatically with a suggested size according to the location of the miss tooth. In Fig.6(a), a pontic is created between two prepared abutment teeth. In Fig. 6(b), two pontics are created according to two prepared abutment teeth.
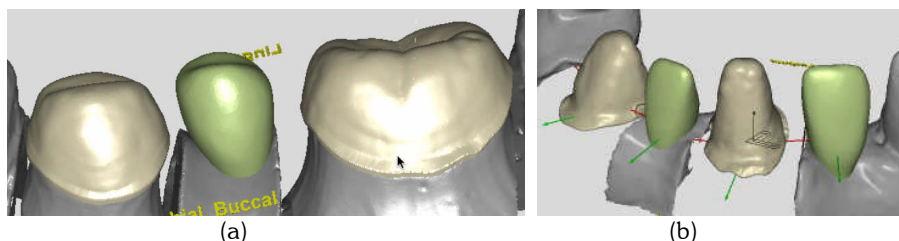


(a)                          (b)

Fig. 6: (a) a pontic is created between two prepared abutment teeth (b) two pontics are created according to two prepared abutment teeth.

### 4.4 Deformation Tool

The deformation tools are needed when the size or shape of coping and pontic models are not correct. The deformation tools include global deformation, wax dropping, and local deformation.

#### 4.4.1 Global Deformation

The FFD (Free-Form deformation) [16] is defined in terms of a tensor product trivariate Bernstein polynomial. Any point $q$ has (s, t, u) coordinates in this system. The deformation is specified by moving the $P_{i,j,k}$ from their undisplaced positions. The deformation function is defined by a trivariate tensor product Bernstein polynomial. The deformed position $q$ of an arbitrary point $q_0$ is found by first computing its (s, t, u) coordinates by using linear algebra, and then evaluating the vector valued trivariate Bernstein polynomial:

$$q(s,t,u) = \sum_{i=1}^{l} \binom{l}{i}(1-s)^{l-i}s^i \left[ \sum_{j=0}^{m} \binom{m}{j}(1-t)^{m-j}t^j \left[ \sum_{k=0}^{n} \binom{n}{k}(1-u)^{n-k}u^k P_{i,j,k} \right] \right] \qquad (3)$$

where $q$ is a vector containing the Cartesian coordinates of the displaced point, and where $P_{i,j,k}$ is a vector containing the Cartesian coordinates of the control point. In Fig. 7, the pontic model is deformed by using the FFD method.
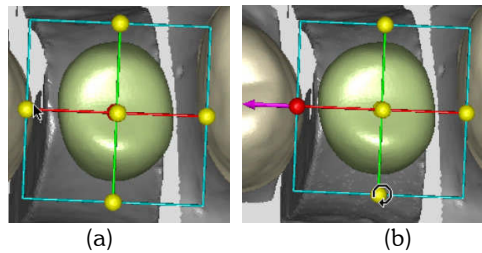


(a)         (b)

Fig. 7: (a) The pontic model before deformation (b) The pontic model after deformation.

#### 4.4.2 Wax Dropping

A density value at a point $q$ on the surface is given by the following equation.

$$q = \sum_{i=0}^{N} w_i f(r_i, R_i) \qquad (4)$$

where $N$ is the number of metaballs, $w_i$ the density at the center of a metaball $i$, $f$ the field function, and $R_i$ the radius of the metaball. And $r_i$ is the distance between the point $P$ and the center position of a metaball, $C_i$, that is, $r_i = |P - C_i|$. The field function is as follows.

$$f(r_i, R_i) = 2 - r_i / R_i \qquad (5)$$

when $r_i < R_i$, otherwise 0. The surface is deformed according to the surface normal and density value. In Fig. 8, after user place some small balls on the surface, the proposed method can deform the surface according to those small balls. Then the smooth operator can make the deformed surface smoother. The deformed result is like we drop wax on the surface.
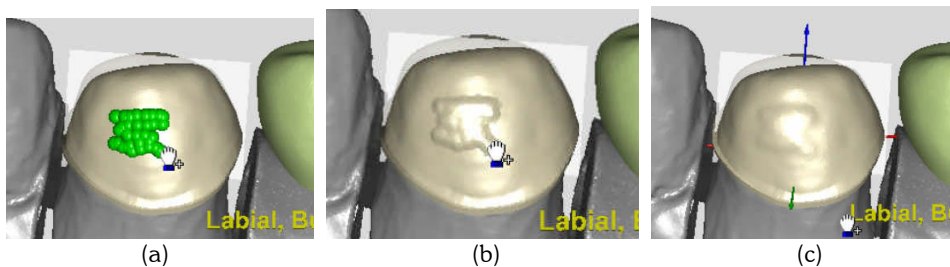


(a)         (b)         (c)

Fig. 8: (a) Put the virtual balls on the selected model (b) The selected area of the coping model are deformed (c) The surface after smoothing.

*4.4.3 Local Deformation*

We use the B-spline basis [17] in stead of the Bernstein polynomials because of the local control properties of B-splines. The deformed position, q, of any arbitrary point with local coordinates, (s, t, u), is given by

$$q_{i,j,k}(s,t,u) = \sum_{l,m,n=-3}^{0} P_{i+l,j+m,k+n} B_l(s) B_m(t) B_n(u) \tag{7}$$

where $P_{i,j,k}$ is the $i^{th}$, $j^{th}$, $k^{th}$ control point in the s, t, and u direction, respectively, and the $B_l(s)$, $B_m(s)$ and $B_n(s)$ are the B-spline blending functions. In Fig. 9, the green area is selected for deformation. The corresponding control points are calculated when the deformation area is selected. The marked control points can be moved manually and the surface will be deformed only in the selected area.
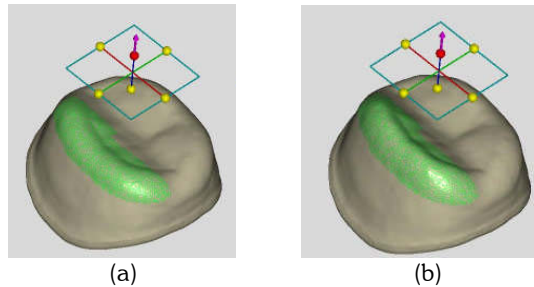


Fig. 9: (a) The coping model before local deformation (b) The coping model after local deformation.

## 4.5 Connector

Each connector surface is calculated by using loft surface algorithm. The connector surface are created with a suggested shape or size. Two boundary curves are projected on the coping and pontic model and the middle curve is a circle or ellipse. The system will use Boolean operator to union coping, pontic and connector into a solid model automatically.
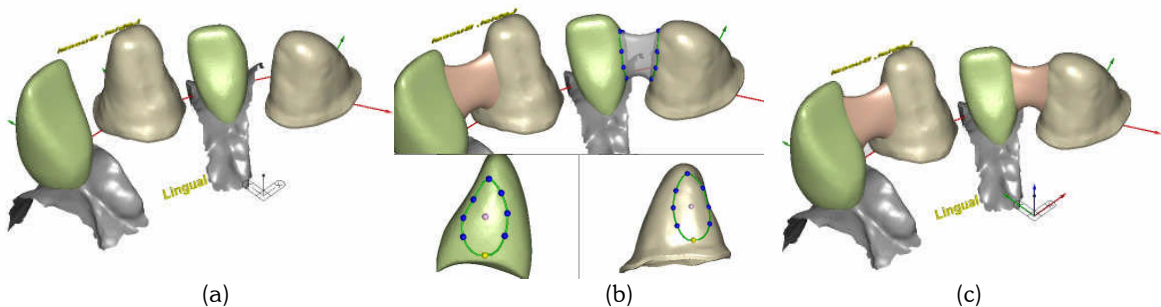


Fig. 10: (a) the coping and pontic model (b) the connector surface is created with a suggested shape or size (c) the bridge coping model.

## 5. RESULTS

In this section, two cases are milled by the ziconia material. Zirconia is strong and has high biocompatibility. Fully sintered zirconia materials can be difficult to mill. Zirconia copings are laminated with low fusing porcelain to provide esthetics and to reduce wear of the opposing dentition. If the abutment lacks adequate reduction the restoration may look opaque. Because they normally are not etchable or bondable, abutments require good retention and resistance form.

## Case 1: Single-unit Coping

In Fig. 11, it takes about 5 minutes to scan and reconstruct the plaster model. In the design process, a single-unit coping takes about 3 minutes to create and modify the model. Finally, the time for CAM and machining is about 15 minutes. The total process takes about 20 minutes. The detail information of triangle number is listed in the Table 1.

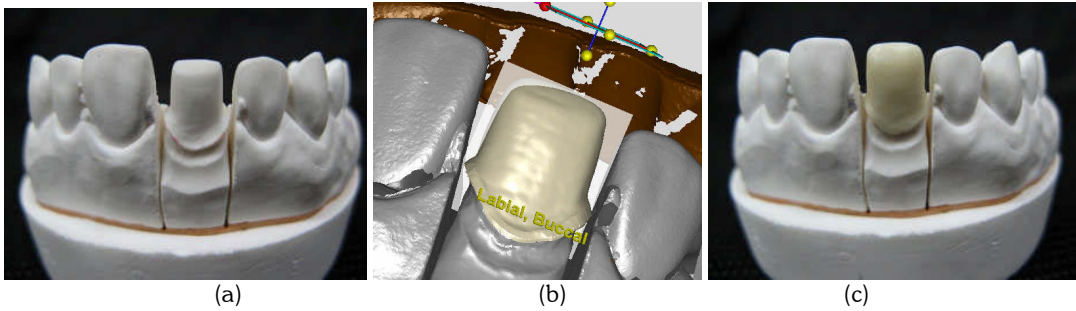(a)                      (b)                     (c)

Fig. 11: (a) the dental plaster model (b) the single-unit coping model is designed in proposed system (c) the coping model is machined by using zirconia material.

**Case 2: Three-unit Coping**

In Fig. 12, it takes about 15 minutes to scan and reconstruct the plaster model. In the design process, a three-unit coping takes about 10 minutes to create and modify the model. Finally, the time for CAM and machining is about 40 minutes. The total process takes about 1 hour. The coping is covered entirely with porcelain as shown in Fig. 13. The detail information of triangle number is listed in the Table 1.



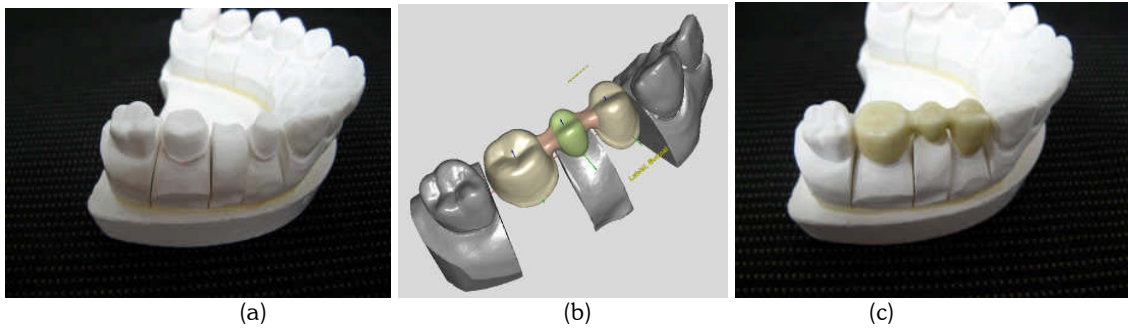(a)                      (b)                     (c)

Fig. 12: (a) the dental plaster model (b) the three-unit coping model is designed in the proposed system (c) the coping model is machined by using zirconia material.



Fig. 13: The dental bridge with porcelain crown.

| Triangle number | Scanned model (n) | Scanned bite model (n) | Coping model (n) | Pontics (n) | Connector (n) | Result model (n) |
|---|---|---|---|---|---|---|
| Case 1 | 37,940 | 101,346 | 43,518 | 0 | 0 | 43,518 |
| Case 2 | 176,480 | 120,680 | 98,320 | 10,589 | 12,328 | 120,157 |

Tab. 1: Detail information of 2 cases.

## 6. CONCLUSION

A customized dental coping design system is proposed in this paper. A structure light optical scanner is used to scan the teeth model. And the registration and triangulation algorithms are used to reconstruct the scanned data to a triangular solid model. The margin lines of the prepared abutment teeth can be detected automatically. The root surface of the abutment teeth can be segmented according to these margin lines. Then the non-uniform offsetting and shelling algorithm is proposed to create the coping shell model with variable thickness. When the size or shape of coping and pontic models are not correct, some deformation tools are proposed to edit the model manually. Finally, the connector will be created between coping and pontic models. In the future, it is possible to extend this system to other dental restorations such as inlays, onlays, crowns, and veneers.

## 7. REFERENCES

[1] Chen, C. S.; Hung, Y. P.; Cheng, J. B. ; A Fast Automatic Method for Registration of Partially-Overlapping Range Images, Proceeding of International Conference on Computer Vision, 1998, 242-248.

[2] Yau, H. T.; Chen, C. Y.; Wilhelm, R. G.: Registration and Integration of Multiple Laser Scanned Data for Reverse Engineering of Complex 3D Models, Int'l Journal of Production Research, 38(2), 2000, 269-285.

[3] Masuda, T.: A Unified Approach to Volumetric Registration and Integration of Multiple Range Images, Proceeding of International Conference on Pattern Recognition, 2, 1998, 977-981.

[4] Masuda, T.; Yokoya, N.: A Robust Method for Registration and Segmentation of Multiple Range Images, Computer Vision and Image Understanding, 61(3), 1995, 295-307.

[5] Zhang, Z.: Iterative Point Matching for Registration of Free-Form Curves and Surfaces, International Journal of Computer Vision, 13(2), 1994, 119-152.

[6] Mencl, E.; Müller, H.: Interpolation and approximation of surfaces from three dimensional scattered data points, State of the Art Reports, Eurographics'98, 1998, 51-67.

[7] Boissonnat, J.-D.: Geometric structures for three-dimensional shape representation, ACM Transactions on Graphics, 3(4), 1984, 266-286.

[8] Edelsbrunner, H.; Mücke E. P.: Three-dimensional alpha shapes, ACM Trans. on Graphics, 13(1), 1994, 43-72.

[9] Adamy, U.; Giesen, J.; John, M.: The $\lambda$-Complex and Surface Reconstruction, Abstracts 16th European Workshop Computer Geometry, 2000, 14-17.

[10] Amenta, N.; Choi, S.; Kolluri, R. V.: The power crust, Proceedings of Sixth ACM Symposium on Solid modeling and applications, Ann Arbor, Michigan, USA, 2001, 249-266.

[11] Yau, H. T.; Kuo, C. C.; Yeh, C. H.: Extension of surface reconstruction algorithm to the global stitching and repairing of STL models, Computer-Aided Design, 35(5), 2002, 477-486.

[12] Kuo, C. C.; Yau, H. T.: Reconstruction of virtual parts from unorganized scanned data for automated dimensional inspection, Journal of Computing and Information Science in Engineering, 3(1), 2003, 76-86.

[13] Hubeli, A.; Gross, M.: Multi-resolution feature extraction for unstructured meshes, Proceedings of the Visualization 2001 Conference, 2001, 287-294.

[14] Guskov, I.; Sweldens, W.; Schröder, P.: Multiresolution signal processing for meshes, In SIGGRAPH '99.

[15] Besl, P. J.; McKay, N. D.: A Method for Registration of 3D Shapes, IEEE Transactions on Pattern Analysis and Machine Intelligence, 14(2), 1992, 239-256.

[16] Sederberg, T. W.; Parry, S. R.: Free-form deformation of solid geometric models, In SIGGRAPH '86 Proceedings, 1986.

[17] Hsu, W. M.; Hughes, John F.; Kaufman, H.: Direct Manipulation of Free-Form Deformations, Computer Graphics, 26(2), 1992, 177-184.

[18] DCS, http://www.dentmed.nl/, President.

[19] Sirona, http://www.sirona.de/, CEREC.

[20] Nobel biocare, http://www.nobelbiocare.com/global/en/default.asp, Pocera system.

[21] Kho, Y.; Garland, M.: Sketching mesh deformations, Proceedings of the 2005 symposium on Interactive 3D graphics and games, 2005, 147-154.

[22] Huang, J.; Shi, X.; Liu, X.; Zhou, K.; Wei, L.; Teng, S.; Bao, H.; Guo, B.; Shum, H.: Subspace gradient domain mesh deformation, ACM Transaction on Graphics, 2006, 1126-1134.

[23] Funck, W.; Theisel, H.; Seidel, H.: Vector field based shape deformations, ACM Transactions on Graphics, 2006, 1118-1125.

[24] Liu, P.: A Panorama of Dental CAD/CAM Restorative Systems, Compendium of Continuing Education in Dentistry, 26(7), 2005, 507-513.